UDC 539.4

Numerical Simulation of Brittle Damage in Concrete Specimens

Y. Labadi[a] **and N. E. Hannachi**[b]

[a] Université de Technologie de Troyes, Troyes, France

[b] Faculté de Génie de la Construction, Université de Tizi-Ouzou, Tizi-Ouzou, Algeria

УДК 539.4

Численное моделирование хрупкого разрушения бетонных образцов

Ю. Лабади[а], **Н. Э. Ханнаши**[б]

[а] Технологический университет г. Труа, Франция

[б] Университет г. Тизи-Узу, Алжир

Предложен критерий повреждения конструкций из бетона, получивший название нормы эквивалентных деформаций, который позволяет учитывать асимметричное механическое поведение бетона при растяжении и сжатии. Разработана изотропная модель, базирующаяся на использовании поверхности повреждения, аналогичной функции течения теории пластичности. С помощью предложенной модели выполнен конечноэлементный расчет нелинейно-упругой деформации образцов из бетона. Проведено сравнение полученных результатов с экспериментальными. Показана хорошая корреляция между расчетными и экспериментальными результатами. Установлено, что точность расчетов более высокая по сравнению с прогнозами, выполненными без применения подходов механики повреждения твердого тела.

Ключевые слова: упругость, повреждение, нелинейное поведение, бетон, конечные элементы, численные методы.

Notations

D – scalar value representing the local damage parameter (ranging from 0 for the virgin material to 1, which represents the failure or zero stress)

ρ_0 – material specific mass

ε_{ij} – strain tensor

σ_{ij} – effective stress tensor

ψ^0 – denotes the initial (undamaged) elastic stored energy

Λ^0_{ijkl} – fourth order tensor of the elastic stiffness of the undamaged material

Λ^s_{ijkl} – fourth order tensor of the elastic stiffness of the damaged material

α – parameter taking into consideration the shear resistance

f_t – material yield stress in tension

f_c – material yield stress in compression

k – coefficient accounting for the large difference in tensile strength and comressive strengths, $k = f_c / f_t$

G_f – fracture energy by unit surface (J/m^2)

g_f – specific fracture energy (J/m^3)

E – Young modulus of the material

G – shear modulus

l_{ch} – characteristic length of the element of volume representing the material's average behavior

Introduction. It is well known that the deformation of most engineering materials is often accompanied by irreversible changes in their internal structure. The nucleation and the growth of distributed microscopic cavities and cracks will not only induce the occurrence of macro-cracks, but also lead to the deterioration of material properties due to internal micro structural changes. Therefore, proper understanding and knowledge of the damaging process and its effects on the macroscopic practical problems are required. An approach to these problems can be provided by the recently developed theory of continuum damage mechanics (CDM), which involves irreversible micro structural changes implicitly. Several types of CDM models have been proposed for brittle materials. For example, the Chow–Yang model [1] is based on the hypothesis of damage surface that is similar to the yield function in plasticity theory and uses one scalar valued internal variable to represent the damage state. The Chaboche model [2] basically assumes anisotropic damage and introduces tensorial damage variables. Therefore, it can be considered that there exists a relationship between small cracks (damage) and strain direction. However, a detailed method to apply this model to anisotropic damage in any direction is still under development. Moreover, CDM theories, which incorporate vectors [3], scalars [4], second-order tensors [5, 6], and fourth-order tensors [7], have been proposed. However, these theories show either a discontinuous stress–strain response when the unilateral condition takes place or an unacceptable non-symmetric elastic behavior for some loading conditions [8]. In this paper, we try to describe the non-linear elastic constitutive equation using CDM and evaluate the structural integrity of brittle material components by the damage parameter introduced in this type of theory. In concrete, the inelasticity is generally associated with irreversible thermodynamics process involving elastic degradation. Strength and stiffness degradation can be effectively modeled in the CDM framework: isotropic damage models with a single damage variable [9] or a tension damage variable and a compression damage variable [10, 11], anisotropic damage models [12, 13], to cite a few.

In this paper, a rather simple isotropic damage model for concrete in the framework for damage mechanics is presented and used to simulate the non-linear elastic deformation behavior of concrete, using the finite element method (FEM). This model introduces a damage surface that is similar to the yield function in the conventional theory of plasticity. A special form of damage surfaces is constructed to illustrate the application of the model. This model contains essentially no adjustable parameters; indeed the damage law requires only the

fracture energy to be completely defined. To verify the FEM program including the present model, the deformations predicted by this model are compared with both the experimental ones in the concrete structural model and the calculated ones without using the CDM; they employed the concept of internal state variables and a phenomenological method to describe the state of a material element. For simplicity, we only consider the rate-independent behavior of the element in an isothermal process. Consequently, time and temperature will not appear in the formulation. The final objective is being able to simulate the behavior of concrete structures until fracture with the relatively simple models of use and implementation. This paper is organized as follows. In Section 1, using the phenomenological approach of continuum damage mechanics; the damage model is formulated into a general framework of the thermodynamics of irreversible processes. The numerical aspects related to the use of this model in finite element analysis are discussed in Section 2. A modified Newton–Raphson algorithm, that uses the initial stiffness matrix as iteration matrix, has been used for the solution of the non-linear system. Finally, numerical results obtained with the presented model are compared with experimental and numerical results concerning the damage development in tension test and on in singleûedge notched concrete beam under bending load.

1. **The Damage Model**.

1.1. ***Energetic Considerations***. The model is formulated in the strain-space, and it is based on the equivalent strain concept. Since the observable variable is the strain and in order to simplify the numerical implementation of this model in finite element code, we choose the Helmholtz free energy as the state potential

$$\psi(\varepsilon_{ij}, D) = [1 - D + (1 - \delta_{ij}\delta_{kl})\alpha D]\left(\frac{1}{2\rho_0}\varepsilon_{ij}\Lambda^0_{ijkl}\varepsilon_{kl}\right), \tag{1}$$

where α is a material parameter varying from 0 (without shear retention) to 1 (damage ineffective for shear stress). It is introduced in order to take into consideration the friction between the two surfaces of crack and it accounts the shear resistance.

As the damage increases towards the unit, the free energy is not equal zero because the shear resistance of cracks. For the energetic consistence of the model, the inequality of Clausius–Duhem that states the no-negative character of the rate of mechanical energy dissipation for any arbitrary infinitesimal variation $\dot{\varepsilon}_{ij}$ from an equilibrium condition has to be ensured

$$\dot{\phi}_D = \frac{1}{\rho_0}\sigma_{ij}\dot{\varepsilon}_{ij} - \dot{\psi} \geq 0. \tag{2}$$

Equation (2) can be written as

$$\dot{\phi}_D = \frac{1}{\rho_0}\sigma_{ij}\dot{\varepsilon}_{ij} - \left(\frac{\partial\psi}{\partial\varepsilon_{ij}}\dot{\varepsilon}_{ij} + \frac{\partial\psi}{\partial D}\dot{D}\right) = \left(\frac{1}{\rho_0}\sigma_{ij} - \frac{\partial\psi}{\partial\varepsilon_{ij}}\right)\dot{\varepsilon}_{ij} - \frac{\partial\psi}{\partial D}\dot{D} \geq 0. \tag{3}$$

Since the variation $\dot{\varepsilon}_{ij}$ is completely arbitrary, this inequality can be fulfilled only if the term in parentheses is identically zero

$$\frac{1}{\rho_0}\sigma_{ij} - \frac{\partial \psi}{\partial \varepsilon_{ij}} = 0. \tag{4}$$

From the Eq. (4) we obtain

$$\sigma_{ij} = \rho_0 \frac{\partial \psi}{\partial \varepsilon_{ij}} = [1 - D + (1 - \delta_{ij}\delta_{kl})\alpha D]\Lambda^0_{ijkl}\varepsilon_{kl} = \Lambda^s_{ijkl}\varepsilon_{kl}. \tag{5}$$

For the normal stresses (i.e., $i = j$ and $k = l$) the term $(1 - \delta_{ij}\delta_{kl})\alpha D$ vanishes in Eq. (5), while for the shear stresses it introduces a reduction of the damage action in order to assure a minimum strength even for the completely damaged material.

Equation (3) can be simplified like follows:

$$\dot{\phi}_D = -\frac{\partial \psi}{\partial D}\dot{D} = \psi^0 \dot{D} \geq 0. \tag{6}$$

This last equation implies the irreversibility of the damage. It is satisfied if D is increasing (that is to say, being always defined positive).

1.2. ***Damage Criterion***. Within the brittle damage approach, the concept of yield surface as the familiar plasticity law is used. There exists a reversible (elastic) domain such that damage does not develop from any interior state but may evolve from a state on the boundary of the domain. So, the damage growth will be governed by a loading surface of equation $f(\varepsilon_{ij}, D) = 0$ (convex in D). This threshold function depends on the equivalent strain and the damage. It is defined in the strain space [6, 9, 12, 14–16]. In this study, a new form for the equivalent strain is proposed. The domain or loading surface is defined as

$$f(\varepsilon_{ij}, D) = \tilde{\varepsilon} - K(\tilde{\varepsilon}, D) \leq 0, \tag{7}$$

where $\tilde{\varepsilon}$ is an equivalent strain or a norm of the strain tensor ε_{ij}, $K(\tilde{\varepsilon}, D)$ is the softening parameter and takes the largest value of $\tilde{\varepsilon}$ ever reached at the considered point in the material. Initially $K(\tilde{\varepsilon}, D) = \varepsilon_{D0}$, in which ε_{D0} is the threshold of damage. Value of ε_{D0} may be regarded as the tensile strain at which damage is initiated. We consider that the threshold is reached when the stress is maximal in uniaxial tension $\varepsilon_{D0} = f_t / E$

$$K(\tilde{\varepsilon}, D) = \max_t \left\lfloor \varepsilon_{D0};\ \max_{\tau \leq t} \tilde{\varepsilon} \right\rfloor. \tag{8}$$

In concrete, there is a large difference in tensile strength and compressive strength. Thus, the following expression is proposed to define the damage

threshold of concrete, taking into consideration the asymmetric behavior in tension and compression:

$$\tilde{\varepsilon} = \left[\frac{[1+r(k-1)]}{k}\right]\sqrt{\left(\frac{1}{2}\right)\underline{\varepsilon}:\underline{J}:\underline{\varepsilon}}, \tag{9}$$

where $\underline{J}$ is a fourth-order symmetrical tensor. For initially isotropic material, $\underline{J}$ may be written as

$$\underline{J} = \frac{1}{\hat{E}}\begin{bmatrix} \frac{1}{E} & \frac{-\nu}{E} & \frac{-\nu}{E} & 0 & 0 & 0 \\ & \frac{1}{E} & \frac{-\nu}{E} & 0 & 0 & 0 \\ & & \frac{1}{E} & 0 & 0 & 0 \\ & & & \frac{1}{G} & 0 & 0 \\ & S & & & \frac{1}{G} & 0 \\ & & & & & \frac{1}{G} \end{bmatrix}, \tag{10}$$

with $\hat{E} = \max(E,G)$, and

$$r = \begin{cases} 0 & \text{if} \quad \sum_{i=1}^{3}|\varepsilon_i| = 0, \\ \dfrac{\sum_{i=1}^{3}\langle\varepsilon_i\rangle}{\sum_{i=1}^{3}|\varepsilon_i|} & \text{if} \quad \sum_{i=1}^{3}|\varepsilon_i| > 0, \end{cases} \tag{11}$$

where ε_i denotes the tensor of principal strains.

1.3. ***Damage Evolution***. While considering a non-standard material, evolution of damage is defined as

$$\dot{D} = \frac{dF(\tilde{\varepsilon})}{d\tilde{\varepsilon}}\left\langle\dot{\tilde{\varepsilon}}\right\rangle. \tag{12}$$

The evolution of damage is governed by an equivalent strain. So that the evolution law writes:

$$\dot{D} = \begin{cases} 0 & \text{if} \quad f(\varepsilon_{ij},D) < 0 & & \text{(unloading)}, \\ \dfrac{dF(\tilde{\varepsilon})}{d\tilde{\varepsilon}}\left\langle\dot{\tilde{\varepsilon}}\right\rangle & \text{if} \quad f(\varepsilon_{ij},D) = 0 & \text{and} \quad \dot{f}(\varepsilon_{ij},D) = 0 & \text{(loading)}, \end{cases} \tag{13}$$

where $dF(\tilde{\varepsilon})/d\tilde{\varepsilon}$ is a positive definite function $\tilde{\varepsilon}$. The shape of the function $F(\tilde{\varepsilon})$ is determined from experimental observations available in the literature [9]. According to [17], the strain–softening curve of concrete must be concave. Then we write $dF(\tilde{\varepsilon})/d\tilde{\varepsilon}$ under exponential form as

$$\frac{dF(\tilde{\varepsilon})}{d\tilde{\varepsilon}} = \left(\frac{\varepsilon_{D0}}{\tilde{\varepsilon}^2}\right)(1 + b\tilde{\varepsilon})\exp[-b(\tilde{\varepsilon} - \varepsilon_{D0})], \tag{14}$$

while proceeding to the integration of Eq. (14) we obtain

$$D = 1 - \left[\left(\frac{\varepsilon_{D0}}{\tilde{\varepsilon}}\right)\exp[-b(\tilde{\varepsilon} - \varepsilon_{D0})]\right], \tag{15}$$

D is defined in the strain interval $[\varepsilon_{D0}, \infty]$, so that for $\tilde{\varepsilon} = \varepsilon_{D0}$ it gives $D = 0$ and for $\tilde{\varepsilon} \to \infty$ it gives $D = 1$. The total energy dissipated during the deformation process has an upper bound value that is equal to the specific fracture energy of the material g_f, can be obtained by the following integration along the whole strain path:

$$g_f = \int_{\varepsilon_{D0}}^{\infty} \sigma(\varepsilon) d\varepsilon = \int_{\varepsilon_{D0}}^{\infty} \psi^0 dD. \tag{16}$$

If we consider a uniaxial test, then $\tilde{\varepsilon} = \varepsilon_{11}$ and $\psi^0 = \dfrac{(\varepsilon_{11}^0)^2}{2\rho_0} E$, and Eq. (16) obtains the following form:

$$g_f = \int_{\varepsilon_{D0}}^{\infty} \frac{(\varepsilon_{11}^0)^2}{2\rho_0} E \frac{dD}{d\varepsilon_{11}^0} d\varepsilon_{11}^0. \tag{17}$$

After some rearrangements, with introducing (15) into (17), the following results are obtained:

$$g_f = \frac{\varepsilon_{D0}^2}{\rho_0} E\left(\frac{1}{2} + \frac{1}{b}\right). \tag{18}$$

Finally b is given like following:

$$b = \left(\frac{g_f \rho_0 E}{f_t^2} - \frac{1}{2}\right)^{-1}. \tag{19}$$

Here b is a dimensionless constant. The relation (19) shows that the parameter b in Eq. (15) depends on the specific fracture energy dissipated during the whole damaging process. The fracture energy per unit surface G_f is defined by $G_f = g_f l_{ch}$. Hence we obtain

$$b = \left(\frac{G_f \rho_0 E}{l_{ch} f_t^2} - \frac{1}{2} \right)^{-1} \geq 0. \tag{20}$$

The value of the fracture energy G_f can be measured during a bending test on notched concrete specimens. Value of G_f is a known material property and l_{ch} is a characteristic length of the element volume representing the material's average behavior. The length l_{ch} characterizes the size of the smallest region over which damage can localize. As is well known, concrete exhibits strain softening leading to a complete loss of strength. In these materials, the secant modulus decreases with increasing strain. At the beginning, a linear relationship between stress and strain exists for up to 60 percent of the maximum stress. Then, micro cracks develop within the specimen, which is indicated by the non-linearity in the curve up to the tensile strength. In the post-peak regime, more micro cracks are developed in the weakest cross section of the specimen called the fracture process zone (FPZ) and they cause a continual decrease of its tensile strength from a peak stress f_t to zero, together with an increase in deformation. More and more micro cracks are formed until finally they coalesce into macro cracks. In the post-peak regime, all fracture energy is consumed in FPZ. This behavior is called strain softening. The characteristic length is a geometrical constant, which is introduced as a measure of the length of the FPZ in a specimen.

Similarly, a uniaxial compression test can be considered and the symbol g_c is adopted to identify the global energy dissipation. We write then

$$b = \left(\frac{g_c \rho_0 E}{f_c^2} - \frac{1}{2} \right)^{-1} \Rightarrow g_c = k^2 G_f. \tag{21}$$

This parameter plays the role of a localization margin that limits the size of the localization zone.

Note that expression (15) is similar to the isotropic damage models given by [9,13, 18] and also to the anisotropic damage models given by [12, 19].

2. **Finite Element Formulation**. The non-linear solution scheme selected in this study uses the secant stiffness matrix at the beginning of the step with combined with a constant stiffness matrix during the subsequent iterations, that is, the incremental-iterative method. A program was written in a FORTRAN code, and is expressed in a modular form consisting of various subroutines called from the main program and from within themselves. It has been written along the same format of elasticity program CALSEF as developed by the International Centre for Numerical Methods in Engineering (CIMNE Barcelona). This software is an adaptation of the PLAST2 program, as developed by Owen and Hinton in their work on finite elements modeling [20]. Also, this program has been adapted for the structural damage analysis by [21]. The same idea has been used in [22] for the 3D damage structures analysis. The preparation of data, as well as the visualization of results, is achieved with the help of the GID (CIMNE) pre-post-processor. The algorithm of calculation is an incremental type, based on the secant method, this type of algorithm is widely used, e.g., [11, 13, 23].

Let's recall some theoretical aspects below. The local equilibrium condition of the continuum can be written as:

on Ω ($i = 1, 3$ and $j = 1, 3$)

$$\partial\sigma_{ij,j} + f_{vi} = 0; \tag{22}$$

on Γ_s

$$\sigma_{ij} n_j = f_{si}, \tag{23}$$

where Ω and Γ_s are the body volume and surface, f_{vi} is the vector of the mass loads, f_{si} is the vector of surface loads, and n_j is the unit vector normal to the surface.

We rewrite the Eq. (22) under a global weak form through the principle of virtual work. We choose an arbitrary virtual displacement $\{u^*\}$ as a test function:

$$-\int_{\Omega} u_i^* \left(\frac{\partial \sigma_{ij}}{\partial x_j} + f_{vi} \right) d\Omega = 0. \tag{24}$$

We proceed then by integrating by parts to get the weak form:

$$\int_{\Omega} \frac{\partial u_i^*}{\partial x_j} \sigma_{ij} d\Omega - \int_{\Gamma} u_i^* f_{si} d\Gamma - \int_{\Omega} u_i^* f_{vi} d\Omega = 0. \tag{25}$$

Under matrix form we write

$$\int_{\Omega} \{\varepsilon^*\}^T \{\sigma\} d\Omega - \int_{\Gamma} \{u^*\}^T \{f_s\} d\Gamma - \int_{\Omega} \{u^*\}^T \{f_v\} d\Omega = 0. \tag{26}$$

While using the stress–strain relation, Eq. (23) becomes

$$\int_{\Omega} \{\varepsilon^*\}^T [\Lambda^s] \{\varepsilon\} d\Omega - \int_{\Gamma} \{u^*\}^T \{f_s\} d\Gamma - \int_{\Omega} \{u^*\}^T \{f_v\} d\Omega = 0. \tag{27}$$

We proceed then with the approximation of the variational form. The domain Ω is divided in subdomains Ω^e (finite elements). The displacements in an element may be approximated as

$$\begin{cases} u_1^e = \sum_{i=1}^{n} N_i(x,y) u_{1i}^e, \\ u_2^e = \sum_{i=1}^{n} N_i(x,y) u_{2i}^e, \\ u_3^e = \sum_{i=1}^{n} N_i(x,y) u_{3i}^e, \end{cases} \tag{28}$$

where N_i are the global shape functions at node i of coordinates (x_i, y_i) in the global reference mark (x, y) and of coordinates (ζ_i, η_i) in the local reference (ζ, η) and n is the number of nodes in the element.

According to the Galerkin method, we use the same approximations for the virtual displacement, so real strains and virtual strains can be written as

$$\begin{cases} \{u(x,y)\} = [N]\{u_n\}, \\ \{\varepsilon(x,y)\} = [B]\{u_n\}, \end{cases} \qquad \begin{cases} \{u^*(x,y)\} = [N]\{u_n^*\}, \\ \{\varepsilon^*(x,y)\} = [B]\{u_n^*\}, \end{cases} \tag{29}$$

where

$$[B_i] = \begin{bmatrix} \dfrac{\partial N_i}{\partial x} & 0 \\ 0 & \dfrac{\partial N_i}{\partial y} \\ \dfrac{\partial N_i}{\partial y} & \dfrac{\partial N_i}{\partial x} \end{bmatrix}$$

for the plane problems

Then we obtain

$$\int_{\Omega^e} [B]^T [\Lambda^s][B] d\Omega^e \{u_n^e\} - \int_{\Gamma^e} [N]^T \{f_s^e\} d\Gamma^e - \int_{\Omega^e} [N]^T \{f_v^e\} d\Omega^e = 0. \tag{30}$$

That conducted to the following elementary shape:

$$[k^{(e)}]\{u_n\} = \{f^{(e)}\}, \tag{31}$$

where $[k^{(e)}] = \int_{\Omega^e} [B]^T [\Lambda^s_{(D)}][B] d\Omega^e$ is the element stiffness matrix and $\{f^{(e)}\} = \int_{\Omega^e} [N]^T \{f_v^e\} d\Omega^e + \int_{\Gamma^e} [N]^T \{f_s^e\} d\Gamma^e$ is the element nodal force,

Assembly of matrixes and elementary vectors provides the global system:

$$\int_{\Omega} [B]^T [\Lambda^s_{(D)}][B] d\Omega \{U_n\} = \int_{\Omega} [N]^T \{f_v\} d\Omega - \int_{\Gamma} [N]^T \{f_s\} d\Gamma. \tag{32}$$

Under condensed form:

$$[K^s(D)]\{U\} = \{F\}, \tag{33}$$

where $[K^S(D)]$ is the global secant rigidity matrix and $\{F\}$ are the global vector forces.

The system of equations (33) is non-linear due to its dependence to the damage parameter D (that is to the stiffness matrix K) on the strain tensor ε (that is on the displacement vector u). Therefore, a step-by-step procedure must

be adopted, where the external loads on the right-hand side of Eq. (33) are applied incrementally. Within each step, the adoption of a regular Newton–Raphson algorithm for the solution of the non-linear system, with the proper tangent stiffness, would provide quadratic convergence to the solution. However, with a full Newton–Raphson scheme the tangent stiffness matrix has to be formed and refactoried for each iteration. Moreover, the tangent stiffness matrix becomes non-symmetric and the computational time drastically increases. In our numerical test, we have found that the adoption of a modified Newton–Raphson scheme requires a computational time, to reach the same tolerance, which is smaller than that required for the full Newton–Raphson scheme. In fact, the greater number of iterations necessary at each time step due to the crudeness of the predictor, is more than counterbalanced by the inversion of the tangent stiffness matrix. Moreover, the modified Newton–Raphson scheme is always convergent to the solution, even in the presence of flex points in the load-displacement curve. With the modified Newton–Raphson algorithm, the iteration scheme for the solution of system (33) becomes:

$$[K^s]\{\Delta U^r\} = \{\Psi(U^r)\}, \tag{34}$$

$$\{U^{r+1}\} = \{U^r\} + \{\Delta U^r\}. \tag{35}$$

Solution of the nonlinear problem will be achieved when the residual force $\{\Psi(U)\}$ ($\{\Psi(U)\} = [K^s(D)]\{U\} - \{F\} \neq 0$) is sufficiently small. At convergence, $\{\Psi(U)\} = \eta$ is a tolerance chosen by the operator (for example, $\eta = 0.001$).

The accuracy of satisfying the global equilibrium equations is controlled by the magnitude of the unbalanced nodal forces. In this study, the convergence criterion employed is the following Euclidean norm:

$$\sqrt{\frac{\sum_{i=1}^{N}(\{\Psi_i^r\})^2}{\sum_{i=1}^{N}(\{f\}_i)^2}} \leq \eta, \tag{36}$$

where N is the total number of degrees of freedom in the case, Ψ is the residual force value, f is the external force acting on the member, r denotes the iteration number, and η is the specified tolerance.

3. **Numerical Applications and Results**.

3.1. ***SENB Specimen (Single-Edge Notched Beam test)***. We carry out a finite element analysis, until the rupture, on plain concrete Iosipescu single-edge specimen, under four-point bending conditions. This type of experiment has been simulated extensively in the literature using experimental [24, 25], analytical and numerical methods [18, 26–30]. Besides, this example is also treated in the examples manual of the commercial finite element software ABAQUS/Explicit [31].

The material properties used in the simulations are chosen as shown in Table 1. The geometry, loads and supports are shown in Fig. 1. The finite element discretization of the specimen is presented in Fig. 2. In the analysis 673 constant strain triangular elements are employed.

T a b l e 1

Mechanical Properties of Concrete for SENB Specimen and Tension Test

Characterictic	SENB Specimen	Tension Test
Young modulus (N/mm^2)	24,800	36,000
Poisson's ratio	0.18	0.15
Uniaxial tensile strength (N/mm^2)	2.8	3.4
Fracture energy (N/mm)	0.05	0.07

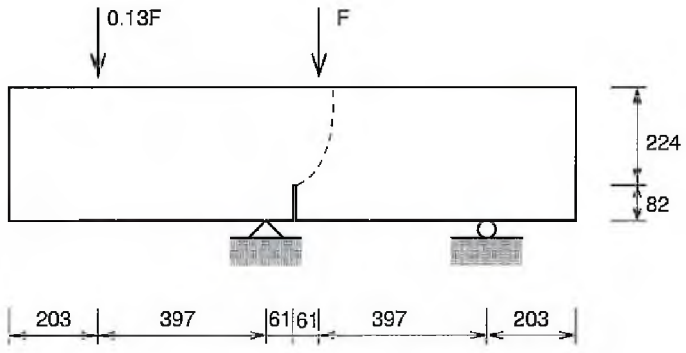

Fig. 1. Single-edge noteched beam: geometry and loading conditions.

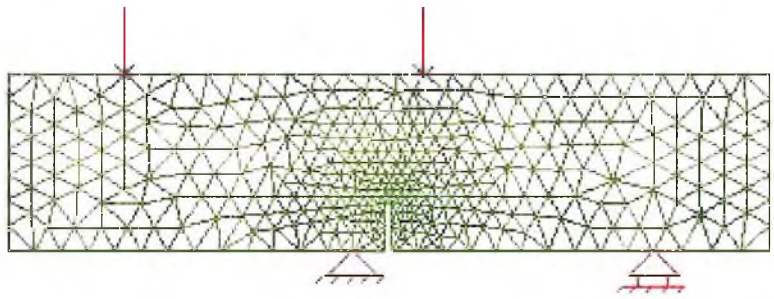

Fig. 2. Mesh used in the analysis for SENB specimen.

In Fig. 3, we present crack pattern of the structure at different instants of this analysis. In Fig. 4, we present a calculation done with a non-local damage model using an adaptive mesh strategy [29]. For a qualitative comparison we refer to the experimental result given in Fig. 5 [25].

With regard to the obtained results, we can see that the damage is localized in a strip, the crack profile corresponds well to the experimental results, and the crack propagates in the predicted direction. The load–CMSD (Crack Mouth Sliding Displacement) curve product by the model (Fig. 6) is comparable with the

one from the experiment [25], and to the one given by [17]. In this test, the behavior is a combination of two modes of fracture. In Fig. 7, we show that the crack opens up in Mode I and in Mode II.

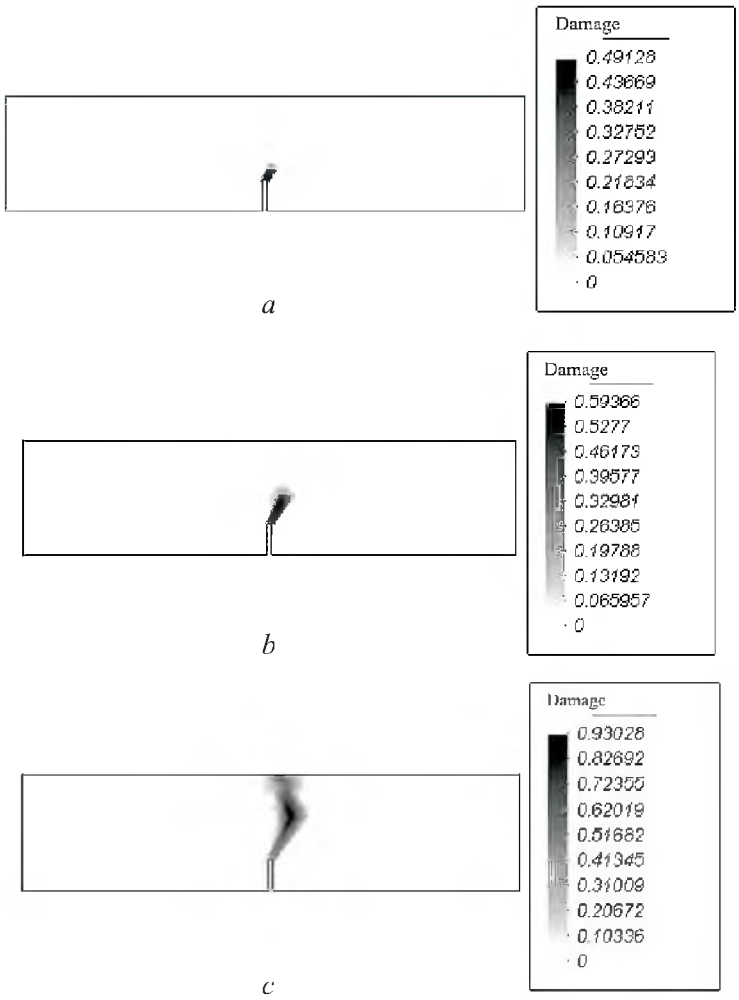

Fig. 3. Damage evolution in a SENB at various instants of the analysis.

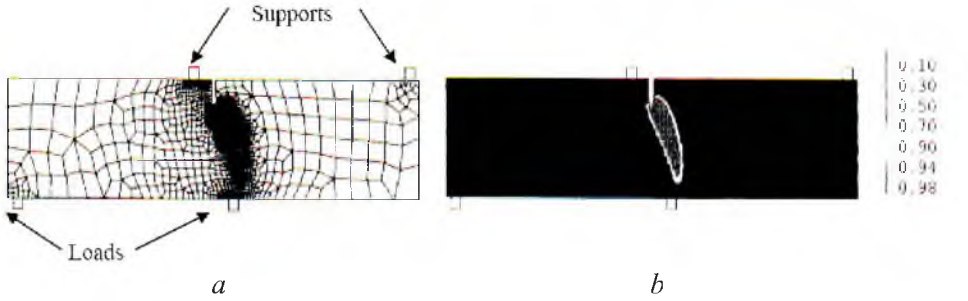

Fig. 4. Crack profile in non local damage analysis (Rodriguez–Ferran et al. 2001): (a) adaptive mesh; (b) damage pattern.

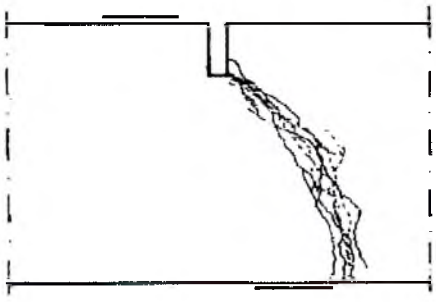

Fig. 5. Experimental crack pattern in SENB (Shlangen 1993).

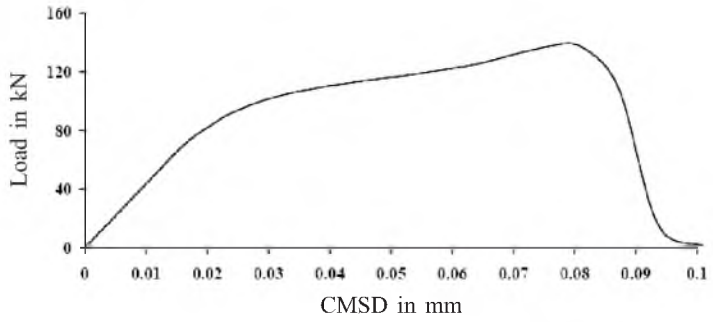

Fig. 6. Load–CMSD curve.

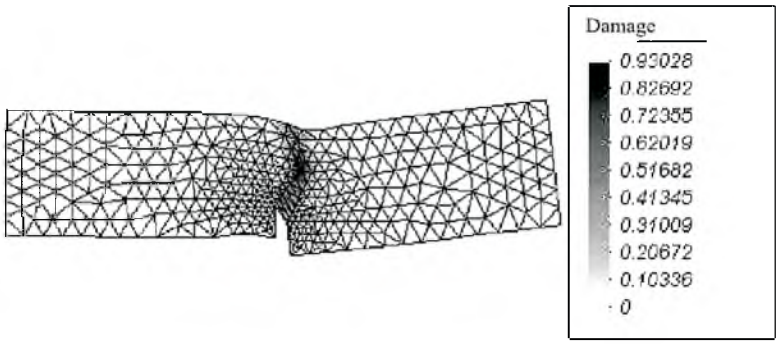

Fig. 7. Final deformed mesh and damage distribution of SENB.

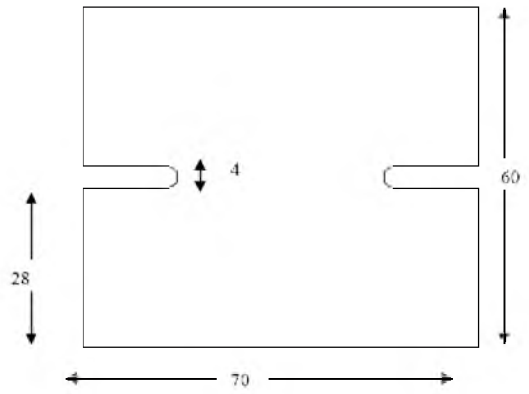

Fig. 8. Tension test: geometrical data (dimensions in mm).

3.2. ***Tensile Test***. This example concerns the simulation of the experimental tension test performed by Hassanzadeh [32] on four edge notched concrete specimen. Di Prisco [33] considered this test as a benchmark. Of this fact, some authors [11, 34] also considered this test. The geometry is shown in Fig. 8. The specimen has been discretised by constant strain triangular elements as shown in Fig. 9. The material properties used in the simulations are chosen as shown in Table 1.

In Fig.10 we present crack pattern of the structure at different instants of the analysis and for a qualitative comparison we consider the numerical results done by Comi [11] as shown in Fig. 11. Finally, the computed total reactions versus the imposed displacement of the top of the specimen are plotted in Fig. 12.

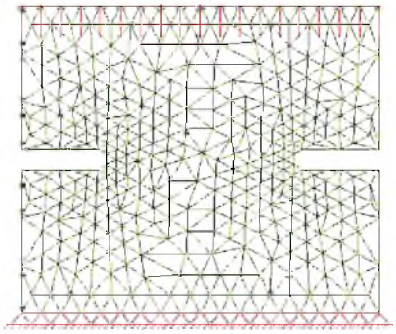

Fig. 9. Tension test: FE mesh and boundary conditions.

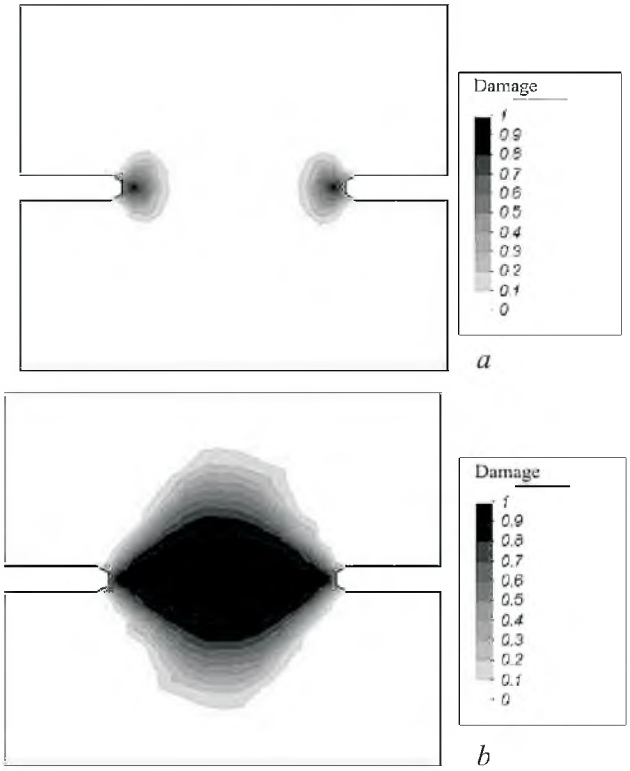

Fig. 10. Predicted damage pattern evolution during the analysis: $u = 0.004$ (a) and 0.05 mm (b).

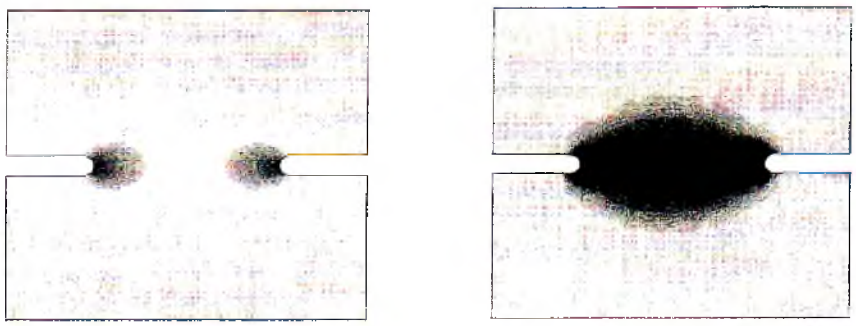

a *b*

Fig. 11. Damage pattern evolution given by Comi: $u = 0.004$ (a) and 0.05 mm (b).

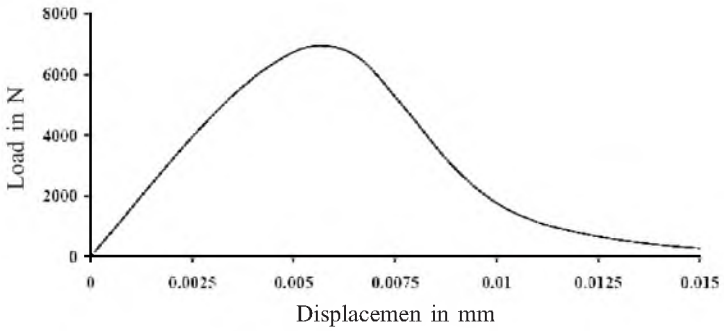

Fig. 12. Load versus displacement under the load point (tension test).

Conclusions. An isotropic damage model for the macroscopic description of concrete behavior, together with its finite element implementation was presented. The damage is directly related to the effective strain through a suitable exponential equation in which a limited number of physically defined material parameters, identifiable by means of standard laboratory tests. Indeed, only one material parameter, that is, the fracture energy, needs to be given together with the classical material mechanical characteristics. The value of the fracture energy can be easily measured by means of a bending test on notched concrete specimens. The damage model and its evolution law in the present work are of particular convenience because of their easy implementation in finite element program and, because the small computational effort that is required in addition to the usual elastic analysis, if a suitable solution scheme is adopted. The form given for the evolution law allows determination of the local damage in direct way and thus allows one to avoid the step-by-step integration of the damage evolution. Due to its simplicity, it is of clear and immediate applicability in existing finite element code. Despite its intrinsic simplicity, it makes possible an effective description of stiffness degradation and strength reduction of the material response. The application of the model to structural analysis predicts satisfactory results and is in good agreement with the experimental data and others numerical results. This model is suitable for the study of quasi-static problems where monotonically increasing loads are applied because the presence of single damage parameter the effect of unilateral effect is not taken into consideration.

Резюме

Запропоновано критерій руйнування конструкцій з бетону, що отримав назву норми еквівалентних деформацій. Критерій дозволяє враховувати асиметричну механічну поведінку бетону при розтязі та стиску. Розроблено ізотропну модель, що базується на використанні поверхні пошкодження, яка аналогічна функції плинності теорії пластичності. За допомогою запропонованої моделі виконано скінченноелементний розрахунок нелінійно-пружної деформації зразків із бетону. Проведено порівняння отриманих результатів з експериментальними. Установлено, що точність розрахунків більш висока, аніж прогнози без використання підходів механіки пошкодження твердого тіла.

1. C. L. Chow and F. Yang, "On one-parameter description of damage state for brittle material," *Eng. Fract. Mech.*, **40**, No. 2, 335–343 (1991).
2. J. L. Chaboche, P. M. Lesne, and J. F. Maire, "Continuum damage mechanics, anisotropy and damage deactivation for brittle materials like concrete and ceramic composites," *Int. J. Damage Mech.*, **4**, No. 1, 5–22 (1995).
3. D. Krajcinovic and G. U. Fonseka, "The continuous damage theory of brittle materials, parts II and I," *J. Appl. Mech. ASME*, **48**, 809–824 (1981).
4. P. Ladeveze and J. Lemaitre, "Damage effective stress in quasi-unilateral material conditions," IUTAM Congress, Lyngby, Denmark (1984).
5. C. Cordebois and F. Sidoroff, "Endommagement anisotrope en élasticité et plasticité," Journal de Mécanique appliquée, **25**, 45–60 (1979).
6. S. Ramtani, "Contribution à la modélisation du comportement multiaxial du béton endommagé avec description de l'effet unilateral," Thèse de doctorat de l'université Paris VI, France (1990).
7. L. W. Ju, "On energy-based coupled elastoplastic damage theories: constitutive modeling and computational aspects," *Int. J. Solids Struct.*, **25**, No. 7, 803–833 (1989).
8. J. L. Chaboche, "Damage induced anisotropy: on the difficulties associated with the active/passive unilateral condition," *Int. J. Damage Mech.*, **1**, 148–171 (1992).
9. J. Lemaitre and J. Mazars, "Application de la théorie de l'endommagement au comportement non linéaire et à la rupture du béton de structure," *Annales de l'ITBTP*, **401**, 114–138 (1982).
10. J. Mazars and G. Pijaudier-Cabot, "Continuum damage theory – application to concrete," *ASCE J. Eng. Mech.*, **115**, No. 2, 345–365 (1989).
11. C. Comi, "A non local model with tension and compression damage mechanisms," *Euro. J. Mech.: A/Solids*, **20**, 1–22 (2001).
12. F. Ghrib and R. Tinawi, "Non linear behavior of concrete dams using damage mechanics," *J. Eng. Mech.*, **121**, No. 4, 513–527 (1995).
13. F. Ragueneau, J. Mazars, and C. La Borderie, "Damage model with frictional sliding. Contributions towards structural damping for concrete structures," *Rev. Euro. Elém. Finis*, **10**, 1–15 (2001).

14. J. W. Dougill, "On stable progressively fracturing solids," *Z. Angew. Math. Phys.*, **27**, No. 4, 423–437 (1976).
15. Z. P. Bazant and S. S. Kim, "Plastic fracturing theory for concrete," *ASCE J Mech.*, **105**, 407–428 (1979).
16. J. C. Simo, J. W. Ju, R. L. Taylor, and K. S. Pister, "On the strain-based continuum damage models: Formulation and computational aspects. Constitutive laws for engineering materials: Theory and applications," C. S. Desai et al. (Eds.), Elsevier Science Publishing (1987).
17. J. G. Rots, "Smeared and discrete representations of localized fracture," *Int. J. Fract.*, **51**, 45–59 (1991).
18. P. H. Feenstra, "Computational aspects of biaxial in plain and reinforced concrete," Ph.D. Thesis, Delft University of Technology, The Netherlands (1993).
19. S. Fichant, G. Pijaudier-Cabot, and C. Laborderie, "Continuum damage modeling: Approximation of crack induced anisotropy," *Mech. Res. Commun.*, **24**, No. 2, 109–114 (1997).
20. D. R. J. Owen and E. Hinton, *Finite Element in Plasticity. Theory and Practice*, Pineridge Press Limited, Swansea, United Kingdom (1980).
21. Y. Labadi, K. Saanouni, and N. E. Hannachi, "Anisotropie induite du dommage avec effet de désactivation/activation," *Annales Maghrébines de l'Ingénieur*, **12**, 671–675 (1998).
22. A. Al-Ghadib, K. Asad-ur-Raman, and M. Baluch, "CDM based finite element code for concrete in 3-D," *Comput. Struct.*, **67**, 451–462 (1998).
23. L. Davenne, C. Saouridis, and J. M. Piau, "Un code de calcul pour la prévision du comportement des structures endommageables en béton, en béton armé, ou en béton de fibres," *Annales de l'ITBTP*, **478**, 139–155 (1989).
24. M. Arrea and A. R. Ingraffea, *Mixed-Mode Crack Propagation in Mortar and Concrete*, Department of Structure Engineering, Cornell University, Report 81-13 (1981).
25. E. Shlangen, "Experimental and numerical analysis of fracture process in concrete," Ph.D. Thesis, Delft University of Technology, The Netherlands (1993).
26. R. De Borst, "Nonlinear analysis of frictional materials," Ph.D. Thesis, Delft University of Technology, The Netherlands (1986).
27. J. G. Rots, "Removal of finite elements in strain-softening analysis of tensile fracture," in: Proc. of the Third Conference on *Computational Plasticity-Fundamentals and Applications*, Pineridge Press (1992), Part I, pp. 669–680.
28. J. Lubliner, J. Oller, S. Oliver, and S. Onate, "A plastic-damage model for concrete," *Int. J. Solids Struct.*, **25**, No. 3, 299–326 (1989).
29. A. Rodriguez-Ferran, I. Arbos, and A. Huerta, "Adaptive analysis based on error estimation for nonlocal damage models," *Rev. Euro. Elém. Finis*, **10**, 193–207 (2001).

30. M. G. D. Geers, R. De Borst, and R. H. J. Peerlings, "Damage and crack modeling in single-edge and double-edge notched concrete beam," *Eng. Fract. Mech.*, **65**, 247–261 (2000).
31. *ABAQUS, User's Manual*, Version 4.8. Hibbit, Karlson and Sorensen, Inc., Palo Ato, California (1990).
32. M. Hassanzadeh, "Behavior of fracture process zones in concrete influenced by simultaneously applied normal and shear displacements," Ph.D. Thesis, Delft University of Technology, The Netherlands (1991).
33. M. Di Prisco, L. Ferrara, F. Meftah, et al., "Mixed mode fracture in plain and reinforced concrete: some results on benchmark tests," *Int. J. Fracture*, **103**, 127–148 (2000).
34. L. Ferrara, "Numerical simulation of mixed-mode fracture in concrete via a non local damage model," in: Proc. of the second Int. PhD Symposium in Civil Engineering (Budapest 26–28 August) (1998), pp. 1–8.

Received 10. 09. 2004